Effect of Chromium on Structure and Tribological Properties of Hydrogenated Cr/a-C:H Films Prepared via a Reactive Magnetron Sputtering System *

Long Liu(刘龙), Sheng-Guo Zhou(周升国)**, Zheng-Bing Liu(刘正兵),
Yue-Chen Wang(王跃臣), Li-Qiu Ma(马利秋)

School of Material Science and Engineering, Jiangxi University of Science and Technology, Ganzhou 341000

(Received 21 September 2015)

Hydrogenated Cr-incorporated carbon films (Cr/a-C:H) are deposited successfully by using a dc reactive magnetron sputtering system. The structure and mechanical properties of the as-deposited Cr/a-C:H films are characterized systematically by field-emission scanning electron microscope, x-ray diffraction, Raman spectra, nanoindentation and scratch. It is shown that optimal Cr metal forms nanocrystalline carbide to improve the hardness, toughness and adhesion strength in the amorphous carbon matrix, which possesses relatively higher nano-hardness of 15.7 GPa, elastic modulus of 126.8 GPa and best adhesion strength with critical load (L_C) of 36 N for the Cr/a-C:H film deposited at CH_4 flow rate of 20 sccm. The friction and wear behaviors of as-deposited Cr/a-C:H films are evaluated under both the ambient air and deionized water conditions. The results reveal that it can achieve superior low friction and anti-wear performance for the Cr/a-C:H film deposited at CH_4 flow rate of 20 sccm under the ambient air condition, and the friction coefficient and wear rate tested in deionized water condition are relatively lower compared with those tested under the ambient air condition for each film. Superior combination of mechanical and tribological properties for the Cr/a-C:H film should be a good candidate for engineering applications.

PACS: 68.55.−a, 81.40.Pq, 81.05.U−, 81.15.Cd DOI: 10.1088/0256-307X/33/2/026801

Diamond-like carbon (DLC) films, having high hardness, low friction coefficient and high wear resistance, biocompatibility and so on, have potential widespread applications in many industrial fields such as windows, magnetic data storage, car parts, field emission display (FED) devices and microelectromechanical devices (MEMs).[1−7] However, a high level of internal stress results in low adhesion and peeling off the films from substrates so that their practical applications are strongly limited.[8] Recently, numerous metal elements, such as Ti, Cr, Ag, W and Al, were often selected to embed into DLC matrixes to reduce internal stress and strengthen film adhesion to the substrate.[9−13] Metallic Cr was reported as an effective element in reducing stress while not deteriorating the superior hardness, friction coefficient, and wear and corrosion resistance of DLC films due to Cr-C nanometer grains or the second phase dispersed in DLC matrixes.[14,15] In general, Cr-DLC films can be deposited by many methods while there should be a great difference in the structure and properties of DLC films deposited by different deposition methods and parameters. Although some reports have discussed the structure and mechanical properties of Cr-DLC films, the effect of CH_4 precursor gas on the microstructure and tribological properties of Cr-DLC films are seldom reported under both the ambient air and deionized water conditions.

In this Letter, the morphology, microstructure and mechanical properties of as-deposited Cr/a-C:H films are characterized systematically, and their friction and wear behaviors are evaluated under both the ambient air and deionized water conditions.

Hydrogenated Cr/a-C:H films were simultaneously deposited on Si wafers and mirror polished stainless steel substrates. Prior to fixing onto the substrate holder in the vacuum chamber, all were ultrasonically cleaned in acetone and ethanol in succession, and then dried in nitrogen blow down. Firstly, the vacuum chamber was pumped to 2×10^{-3} Pa, and then the pure Cr interlayer was deposited to improve the adhesion strength between films and the substrates. Lastly, the hydrogenated Cr/a-C:H films were deposited by sputtering two Cr targets (purity>99.99 wt.%) in CH_4 and Ar mixed gas atmosphere. The deposition parameter of Cr interlayer was described as follows: temperature of 200℃, Cr target power of 200 W, pressure of 3 Pa, Ar flow rate of 60 sccm and deposition time of 30 min. The deposition parameter of Cr/a-C:H films was described as follows: Cr target power of 140 W, Ar flow rate of 50 sccm, pressure of 2 Pa, the negative bias voltages of −300 V, deposition time of 90 min, the CH_4 flow rate varying from 16 to 24 sccm (16, 18, 20, 22 and 24 sccm, respectively), and there was no extra-heating to the substrates.

The structure of hydrogenated Cr/a-C:H films was characterized by x-ray diffraction (XRD) (Bruker D8 x-ray facility), field emission scanning electron microscopy (FESEM) (Hitachi S4800) and Raman spectroscopy (HR800). The mechanical properties including hardness and adhesion strength were evaluated by using the MTS Nano-Indenter G200 system and a Revetest CSM scratch tester, respectively. The friction and wear behaviors of the Cr/a-C:H films were

*Supported by the National Natural Science Foundation of China under Grant Nos 51302116 and 51365016, and the Open Fund Item of State Key Laboratory of Solid Lubrication of Lanzhou Institute of Chemical Physics of Chinese Academy of Sciences under Grant No LSL-1203.

**Corresponding author. Email: zhousg@jxust.edu.cn

© 2016 Chinese Physical Society and IOP Publishing Ltd

evaluated on the Rtec tribometer (USA) reciprocating sliding tribometer under both the ambient air condition and the deionized water condition. The Si_3N_4 ball with a diameter of 3 mm was used as the counter body, and all frictional tests were performed under a load of 5 N with the amplitude of 5 mm and sliding speed of 20 mm/s. The wear rates obtained after the sliding tests were completed on the base of the wear track depth profiles detected by an Alpha-Step IQ profilometer.

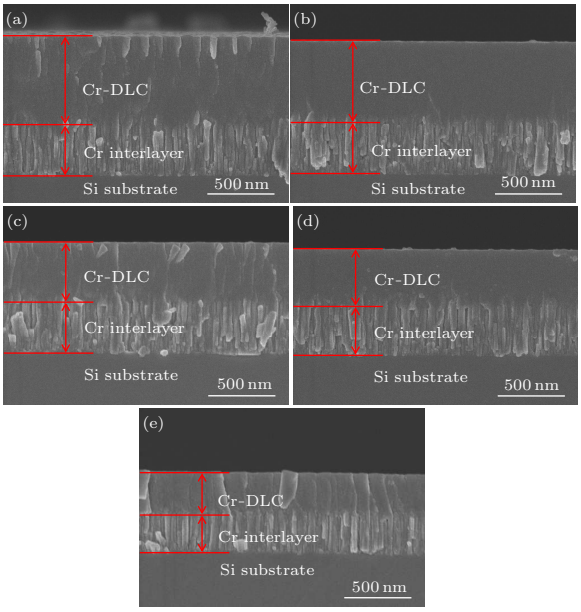

Fig. 1. Cross-sectional morphology of the Cr/a-C:H films deposited at different CH_4 flow rates: (a) 16 sccm, (b) 18 sccm, (c) 20 sccm, (d) 22 sccm and (e) 24 sccm.

The cross-sectional morphology of Cr/a-C:H films at different CH_4 flow rates was observed by an FE-SEM. As can be seen in Fig. 1, all pure Cr interlayers were characterized by columnar structures between as-deposited film and the substrate, and it did not suffer from any apparently localized delaminations between interfaces. In particular, the as-deposited films show relatively dense and homogenous structure in different CH_4 flow rates. Moreover, the thickness of the Cr/a-C:H films was decreased from 661 nm to 314 nm as the CH_4 flow rate was increased from 16 sccm to 24 sccm. XRD revealed the phase in the Cr/a-C:H films, and the corresponding results are depicted in Fig. 2 (a). The diffraction peaks at 33.2°, 44.7° and 61.9° were attributed to $Cr_3C_2(201)$, $Cr_3C_2(204)$ and $Cr_3C_2(215)$. Due to the internal compressive stress, all peak positions could be shifted toward lower 2θ angles compared with the ICDD positions.[16] Furthermore, Raman spectroscopy was used to investigate the influence of CH_4 flow rate on the bonding of DLC matrix, as shown in Fig. 2 (b). It can be seen that all Raman spectra show an asymmetrical broad peak with a shoulder peak, and the intensities of the peaks were apparently enhanced with the increase of CH_4 flow rate. Also, the intensity ratios of G and D bands (I_D/I_G) were obtained by Gaussian deconvolution peaks, Fig. 3 (a) shows the G peak position and I_D/I_G ratio of the Cr/a-C:H films as a function of the CH_4 flow rate. The peak position of G band shifts slightly from 1535 to 1534 cm^{-1} in a small range, and I_D/I_G decreases from 0.88 to 0.82 with the increase of the CH_4 flow rate, indicating an increase of the fraction of sp^3 in the Cr/a-C:H films.

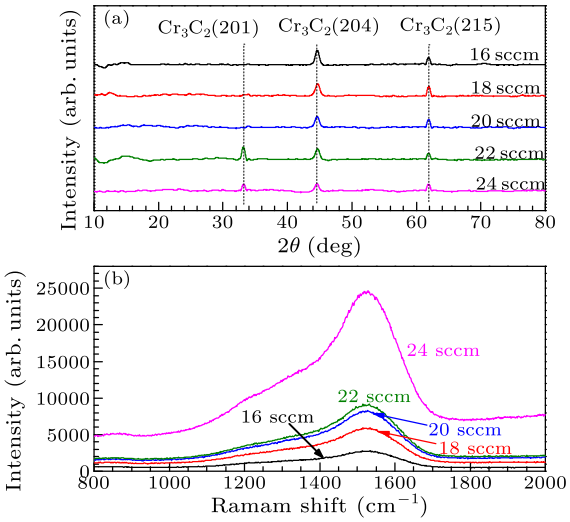

Fig. 2. XRD patterns (a) and Raman spectra (b) of the Cr/a-C:H films deposited at different CH_4 flow rates.

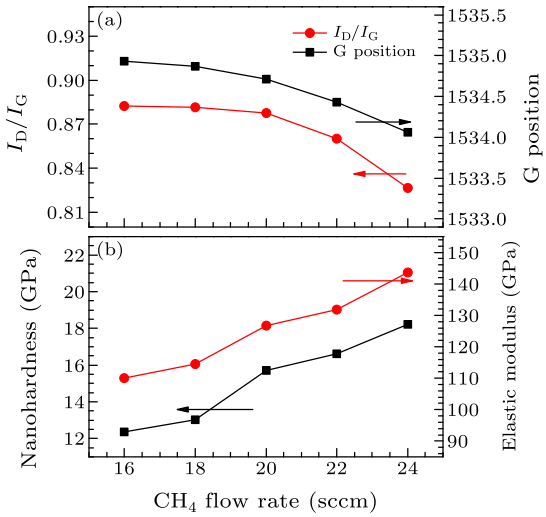

Fig. 3. The G peak position and I_D/I_G ratio (a) and mechanical properties (b) of the Cr/a-C:H films as a function of the CH_4 flow rate.

The hardness (H) and elastic modulus (E) of as-deposited Cr/a-C:H films versus CH_4 flow rate are shown in Fig. 3(b). It can be seen that as-deposited films can achieve relatively good mechanical properties. With the variety of CH_4 flow rate, the hardness and elastic modulus nearly change monotonously which fluctuate from 12.3 GPa and 114.1 GPa to 18.2 GPa and 143.6 GPa. Furthermore, the adhesion strength of as-deposited Cr/a-C:H films was evaluated by a scratch tester, and the critical load (L_C) gained via the acoustic emission curves are as follows: 28 N (16 sccm), 34 N (18 sccm), 36 N (20 sccm), 31 N

(22 sccm) and 26 N (24 sccm), and the Cr/a-C:H film deposited at CH_4 flow rate of 20 sccm presents the optimal adhesion strength. Also, the optical images of scratch tracks of the films deposited on stainless steel substrates at different CH_4 flow rates are shown in Fig. 4. It can be seen that the effect of CH_4 flow rate on the fracture behavior of the as-deposited film is obvious. More cracks and abruptly localized delamination of brittle characteristic appeared in the track of the Cr/a-C:H films deposited at relatively higher or lower CH_4 flow rate. In all, the Cr/a-C:H film deposited at CH_4 flow rate of 20 sccm can possess good combining mechanical performance compared with others.

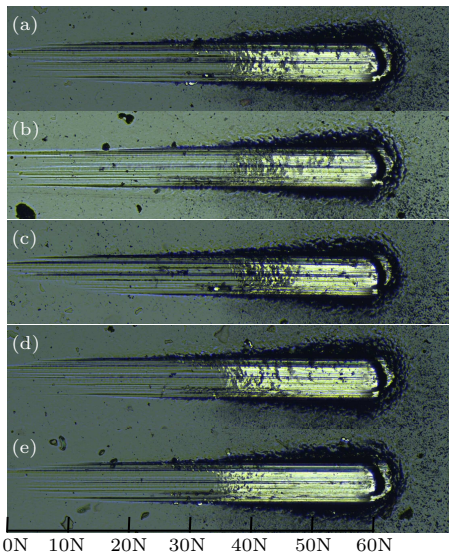

Fig. 4. The scratch tracks of the Cr/a-C:H films deposited at different CH_4 flow rates: (a) 16 sccm, (b) 18 sccm, (c) 20 sccm, (d)22 sccm, and (e) 24 sccm.

The evolution of the friction coefficients as a function of sliding time tested in ambient air condition for as-deposited Cr/a-C:H films is shown in Fig. 5(a), and the corresponding wear tracks were detected by a profilometer and their wear rates can be calculated. Apparently, the friction and wear behaviors of the films depend on the CH_4 flow rate. The results show that the friction coefficient and the wear rate of the films slightly change from 0.13 and 12.9×10^{-7} mm^3/Nm to relatively lowest values of 0.08 and 7.6×10^{-7} mm^3/Nm as the CH_4 flow rate increases from 16 to 20 sccm, while the friction coefficient and the wear rate reversely increase as the CH_4 flow rate increases continuously. Moreover, it can be noticed that it can reach a relatively smooth and stable curve after a short running-in for the Cr/a-C:H film deposited at the CH_4 flow rate of 20 sccm whereas the curves present a more fluctuating feature for the other films. Furthermore, the morphologies of wear tracks and their corresponding wear scars tested in ambient air are characterized by SEM, as shown in Fig. 6. It is illustrated that the wear track presents as a relatively more smooth and shallow one for the Cr/a-C:H film deposited at the CH_4 flow rate of 20 sccm whilst its corresponding wear scar on the sliding ball is also relatively small. However, the other Cr/a-C:H films show relatively more serious wear surfaces. In particular, a mass of wear debris can be found for the films deposited at lower CH_4 flow rate.

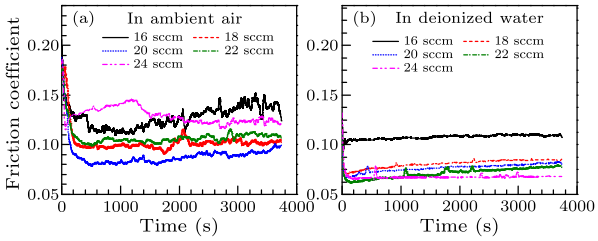

Fig. 5. Friction coefficients of the Cr/a-C:H films as a function of sliding time tested in ambient air (a) and in deionized water (b).

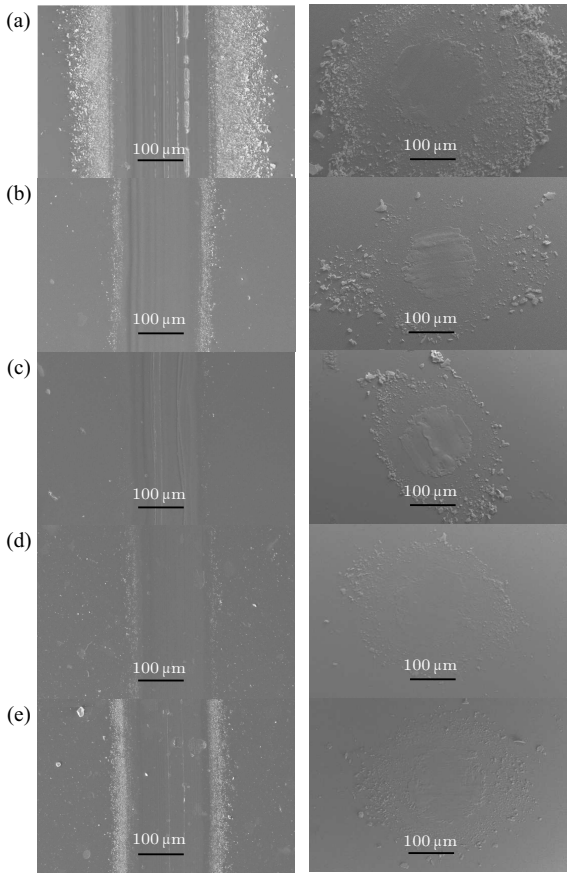

Fig. 6. Wear tracks (left) and wear scars (right) of the Cr/a-C:H films deposited at different CH_4 flow rates tested in ambient air: (a) 16 sccm, (b) 18 sccm, (c) 20 sccm, (d) 22 sccm, and (e) 24 sccm.

In addition, the evolution of the friction coefficients as a function of the sliding time tested under the deionized water condition for as-deposited Cr/a-C:H films is shown in Fig. 5(b) whilst their corresponding wear rates are calculated. The results obviously show that each friction coefficient of the films tested under the deionized water condition is relatively lower compared with that tested under the ambient air condition whilst its corresponding wear rate tested under the deionized water condition is also lower than

that tested under the ambient air condition. Particularly, it is relatively smooth and stable for the curves of friction coefficients of all as-deposited Cr/a-C:H films. However, the changing trend of the friction and wear is different compared with the feature tested in ambient air, and the friction coefficient and wear rate of the films decrease from higher value (0.11 and 11.5×10^{-7} mm^3/Nm) to lower value (0.06 and 5.9×10^{-7} mm^3/Nm) as the CH_4 flow rate increases from 16 sccm to 24 sccm that should be related to the water lubrication and structure of the films. Meanwhile, the morphologies of wear tracks of the Cr/a-C:H films and their corresponding wear scars tested under the deionized water condition are characterized by SEM, as shown in Fig. 7. It is shown that a relatively deep and broad wear track as well as a large wear scar can be observed for the film deposited at CH_4 flow rate of 16 sccm. With the increase of the CH_4 flow rate, wear tracks become smoother and shallower, and wear scars also become smaller. In particular, the contact frictional surfaces on the ball counterparts tested under the deionized water condition are less covered with transferred materials compared with the results tested in ambient air.

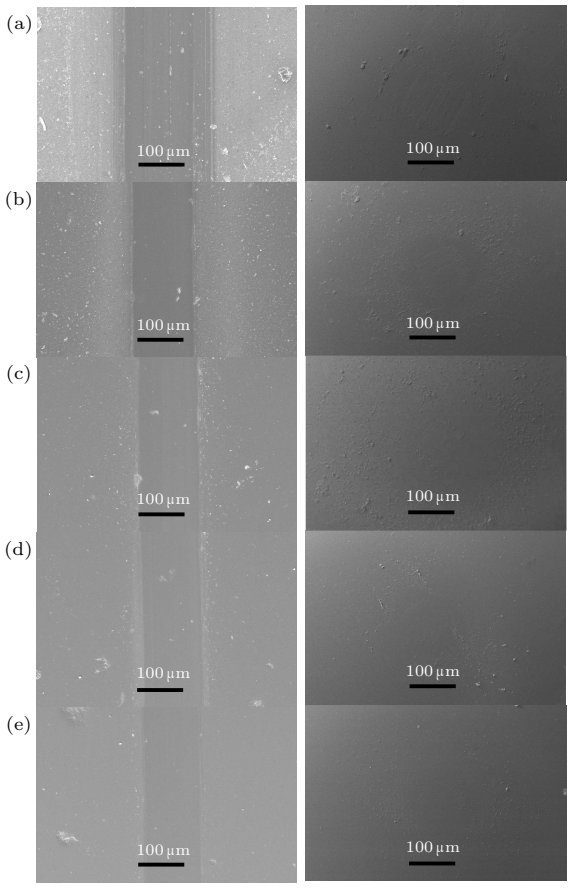

Fig. 7. Wear tracks (left) and wear scars (right) of the Cr/a-C:H films deposited at different CH_4 flow rates tested in deionized water: (a) 16 sccm, (b) 18 sccm, (c) 20 sccm, (d) 22 sccm, and (e) 24 sccm.

Considering the above results, it can be understood that the chromium content in the as-deposited films fundamentally depends on the CH_4 flow rate into the vacuum chamber so that it significantly affects the structure, mechanical and tribological properties of the films. Under the condition of metallic Cr and CH_4 gas hybrid reaction, the target surface dynamic variety between covering by carbonaceous species and cleaning the metallic Cr target should contribute to understanding the evolution of composition as a function of the CH_4 flow rate. In the case of relatively lower CH_4 flow rate, the target collision with Ar^+ is strong so that a large amount of metallic Cr atoms can be easily sputtered from the target surface, and then the 'target poisoning', in which the target was covered gradually by carbonaceous species, would become more serious as the CH_4 flow rate increases to result in an increase of carbon content and decrease of Cr content in the as-deposited films.[17] XRD patterns confirm that the nanocrystallites of chromium carbide are formed in the Cr/a-C:H films, and the evolution of diffraction peaks indicates that the fraction of the chromium carbide decreases as the CH_4 flow rate increases. No carbon and diamond diffraction peak is detected, indicating that the matrix of the films is amorphous. Smaller I_D/I_G ratio and lower G site could correspond to higher sp^3 content in the Cr/a-C:H films, as shown in Fig. 3(a). These indicate that the Cr in form of metallic carbide can induce the transformation of sp^3 to sp^2, causing the graphitization of films.[18] In general, the hardness of DLC films mainly depends on the sp^3 carbon interlink matrix, thus it results in a decrease of hardness as the CH_4 flow rate changes from 24 to 16 sccm. In addition, the formation of Cr–C or metal nano-cluster phase could break up the continuity of carbon network. However, the Cr incorporation can relax the internal stress and might cause the plasticity of the as-deposited films. The metal atoms distributing in the amorphous carbon matrix play a role of a pivotal site, whereby distortion of the atomic bond angles can occur without inducing a significant increase in the elastic energy, and then the internal stress can be relaxed through the atomic bond distortion. Furthermore, the Cr–C bond length is longer than the C–C bond length, and it should also cause the increase of the internal stress.[19] Therefore, an optimal Cr content should be the best improvement to the combination of mechanical properties of the Cr/a-C:H films. Scratch testing results present that it can achieve the highest critical load (L_C) for the Cr/a-C:H film deposited at the CH_4 flow rate of 20 sccm whilst its scratch track presents less brittle cracks and abruptly localized delamination. Consequently, the Cr/a-C:H film deposited at CH_4 flow rate of 20 sccm can possess good combining mechanical performance with relatively high hardness as well as high adhesion strength.

The friction and wear behaviors could be mainly correlated with structure and mechanical properties of films. The Cr/a-C:H film deposited at CH_4 flow rate of 20 sccm showed a relatively stable friction–distance profile and smooth wear under the ambient air condition while the Cr/a-C:H films deposited at lower or higher CH_4 flow rate present more fluctuating fric-

tional curves and serious wear. In the case of low CH_4 flow rate, the worse friction and wear behaviors should be attributed to much more metallic chromium that would significantly cause a rougher surface, lower hardness and adhesion strength, and in the case of high CH_4 flow rate, it should be attributed to much less metallic chromium that would cause high internal stress and low adhesion strength. Moreover, the superior friction and wear behaviors of Cr/a-C:H film deposited at CH_4 flow rate of 20 sccm might be attributed to the low shear strength graphitic interlayer (transfer layer) induced by localized rising temperature at asperity contacts under the ambient air condition, as shown in Fig. 6. Also, the friction and wear behaviors of the Cr/a-C:H films are tested under the deionized water condition, and it is found that the friction coefficient and wear rate tested under the deionized water condition are lower than those tested under the ambient air condition for each single Cr/a-C:H film. These should be attributed to the deionized water having an effectively hydraulic lubricating effect. In addition, the density of films could profoundly affect the wear behaviors under the deionized water condition, which might be the main reason that the friction and wear behaviors of films could become better with the increase of the CH_4 flow rate. In all, it can achieve superior combination of mechanical and tribological properties for the Cr/a-C:H film with optimal Cr component under both the ambient air and water conditions, which should become a good candidate for engineering applications.

In summary, hydrogenated Cr/a-C:H films have been successfully fabricated and the characterization shows that optimal Cr metal formed nanocrystalline carbide to improve the hardness, toughness and adhesion strength in the amorphous carbon matrix for the Cr/a-C:H film deposited at CH_4 flow rate of 20 sccm. Also, it can achieve low friction and anti-wear performance for the Cr/a-C:H film deposited at CH_4 flow rate of 20 sccm under the ambient air condition. The friction coefficient and wear rate tested under the deionized water condition are relatively lower compared with that tested under the ambient air condition for each Cr/a-C:H film. Superior combination of mechanical and tribological properties for the as-deposited film with optimal Cr component under both the ambient air and water conditions should be a good candidate for engineering applications.

References

[1] Ding X L, Li Q S and Kong X H 2009 *Chin. Phys. Lett.* **26** 027802
[2] Bai S Y, Tang Z A, Huang Z X, Yu J, Wang J and Liu G C 2009 *Chin. Phys. Lett.* **26** 076601
[3] Liu A P, Liu M, Yu J C, Qian G D and Tang W H 2015 *Chin. Phys.* B **24** 056804
[4] Wang C B, Shi J, Geng Z R, Zhang J Y et al 2012 *Chin. Phys. Lett.* **29** 056201
[5] Fu D, Xie D, Zhang C H, Zhang D, Niu J B, Qian H and Liu L T 2010 *Chin. Phys. Lett.* **27** 098102
[6] Zhang P Z, Li R S, Pan X J and Xie E Q 2013 *Chin. Phys.* B **22** 058106
[7] Ogwu A A, Okpalugo T I T and McLaughlin J A D 2012 *AIP Adv.* **2** 032128
[8] Zhang C Z, Tang Y, Li Y S and Yang Q 2013 *Thin Solid Films* **528** 111
[9] Dai W, Ke P L, Moon M W, Lee K R and Wang A Y 2012 *Thin Solid Films* **520** 6057
[10] Manninen N K, Ribeiro F, Escudeiro A, Polcar T, Carvalho S and Cavaleiro A 2013 *Surf. Coat. Technol.* **232** 440
[11] Zhou S G, Wang L P, Lu Z B, Ding Q, Wang S C, Wood R J K and Xue Q J 2012 *J. Mater. Chem.* **22** 15782
[12] Pu J B, Zhang G A, Wan S H and Zhang R H 2015 *J. Compos. Mater.* **49** 199
[13] Wei X L, Zhang G A and Wang L P 2015 *Tribol. Lett.* **59** 1
[14] Zou C W, Wang H J, Feng L and Xue S W 2013 *Appl. Surf. Sci.* **286** 137
[15] Singh V, Jiang J C and Meletis E I 2005 *Thin Solid Films* **489** 150
[16] Zhang S, Xie H, Zeng X T and Hing P 1999 *Surf. Coat. Technol.* **122** 219
[17] Dai W, Wu G S and Wang A Y 2010 *Diamond Relat. Mater.* **19** 1307
[18] Wu Z Z, Tian X B, Gui G, Gong C Z, Yang S Q and Chu P K 2013 *Appl. Surf. Sci.* **276** 31
[19] Li X W, Ke P L and Wang A Y 2015 *J. Phys. Chem.* C **119** 6086